Notas Técnicas do
Laboratório Nacional de Astrofísica

PanEOS
A first data characterization

Albert Bruch

LNA/NT/2016-12
April/2016

PanEOS
A first data characterization

Albert Bruch
Laboratório Nacional de Astrofísica

2016, April 29

Abstract: PanEOS is a system for the detection of space debris which is currently being installed at OPD. It will take white light images of a significant part of the sky visible from the observatory at a high cadence. These data will be available also for research in astronomy. On the bases of sample data from another already operational PanEOS station this contributions characterizes some of the important properties of the images in order to provide a first idea of their usefulness for astronomical purposes. In view of the limited amount of available data and in particular due to the as yet unkown operational procedures for PanEOS at OPD this study can only be considered as a first step towards a more thorough assessment of this question.

Key words: Instrument characterization

1 Introduction

In the context of an agreement between Laboratório Nacional de Astrofísica (LNA) and the Russian Space Agency ROSCOSMOS an "Optical-Electronic Complex for Detection and Measurement of the Movement Parameters of Space Debris" (OEC DSD), also known as "PanEOS" (abbreviation to be used throughout this document), is currently being installed at the Observatory do Pico dos Dias (OPD). This is worldwide the second of a system of similar installations which ROSCOSMOS plans to build in future years, the first one being already operational in the Altay mountains in central Asia.

PanEOS consists of several wide field telescopes mounted on the same mounting. The main telescope has an aperture of 75 cm. It is complemented by two 25 cm telescopes and two 13.5 cm telescopes. The operational mode is such that the telescope will monitor a large portion of the visible sky in white light, concentrating on regions where space debris is expected to be concentrated. This includes, but is not restricted to, a belt of $\pm 15^{\circ}$ around the equator. Ideally, the entire region of interest will be covered once every clear night.

While the main purpose of PanEOS is the detection and monitoring of space debris, it is obvious that the images delivered by the system will also contain a wealth of astronomical information. The contract signed by LNA foresees that Brazilian scientists as well as foreign scientist affiliated to Brazilian institutions will have access to the data collected by PanEOS. In recent contacts with the Russian partners they also signaled that LNA and thus the Brazilian astronomical community might also use some dedicated time at the telescope. It is therefore of interest to characterize the images provided by the system in order to assess their usefulness for astronomical research.

This technical note is meant as a first step in this directions. It is based on data put at the disposal of LNA by the Russian partners, originating from the above mentioned already existing PanEOS station in the Altay mountains. Considering that LNA does not yet have

Table 1: Available data

Telescope	No. of Images[1]	Exposure time (s)
75 cm	10	2
	10	4
	10	5
	10	8
25 cm	10	8
	10	10

[1]The images of a series have been taken in immediate succession.

detailed information about operational procedures and the specific instrumentation planned for PanEOS at OPD, the present data characterization must be considered preliminary.

2 Data

The present study draws on the data detailed in Table 2. Here, I will restrict myself to an analysis of the images taken with the 75-cm telescope with exposure times of 8^s and of the 25-cm telescope exposed for 10^s. When evaluating the results it should always be kept in mind that the exact instrumentation which will be installed at OPD may (and probably will) have somewhat different characteristics compared to those of the PanEOS station which gave origin to the presently available data. Therefore, they should be regarded *cum granum salis*.

As mentioned, details of the operational procedures are not yet known. On the bases of the currently available data it may be conjectured that PanEOS usually takes several images with short exposure times of the same stellar field in immediate succession. This makes sense when searching for space debris which is expected to move on the sky between the individual exposures.

It is not known whether or not basic calibration procedures such as bias subtraction or flat-fielding have been applied to the images. The "sky background" in all images has a rather high values of several thousand ADU units. This permits the suspicion that no bias subtraction has been performed (and then probably also no flat-fielding). However, a considerable contribution of background light cannot be excluded because the observations, performed on 2014, June 12, were obtained just one day before full moon.

All images are given in FITS format. The header contents differ slightly between data for the 75 cm and the 25 cm telescopes. An example of the header of a 75 cm telescope image is shown in Table 2. The 25 cm telescope data header contains the same keywords except for CCDNUM, SAONUM, OPENBEG, OPENEND, CLOSEBEG, CLOSEEND, and MREVERSE which are missing.

3 75-cm telescope data

3.1 General characteristics

Fig. 1 shows a single 8 sec exposure of Selected Area SA-18, centred on RA = $21^h\ 27^m\ 8^s$ and Dec = 60^o 32' 40". The image has a size in pixels of 2080 columns × 4612 lines.

Table 2: Example of a FITS image header of the 75-cm telescope

SIMPLE	=	T	/ Standard FITS file
BITPIX	=	16	/ No. of bits per pixel
NAXIS	=	3	/ No. of axes in matrix
NAXIS1	=	2080	/ No. of pixels in X
NAXIS2	=	4612	/ No. of pixels in Y
NAXIS3	=	1	/ No. of images
CRVAL1	=	0	/ Offset in X
CRVAL2	=	0	/ Offset in Y
ORIGIN	=	'Sight$_M$ SAO RAS'	/ ACQUSITION SYSTEM
DATE-OBS	=	'2014-06-12'	/ DATE (YYYY-MM-DD) OF OBS.
TIME-OBS	=	'21:12:39.16309'	/ TIME (hh:mm:ss.sssss) OF OBS.
TELESCOP	=	'Sova-75 0'	/ TELESCOPE NAME
INSTRUME	=	'10391'	/ INSTRUMENT
OBSERVER	=	' '	/ OBSERVERS
OBJECT	=	' '	/ NAME OF IMAGE
BSCALE	=	1.00	/ REAL = TAPE*BSCALE + BZERO
BZERO	=	32768.0	/
DATAMAX	=	57168.0	/ MAX PIXEL VALUE
DATAMIN	=	1.0	/ MIN PIXEL VALUE
FILE	=	'sa18$_0$37$_6$.fts'	/ original name of input file
IMAGETYP	=	'obj'	/ object, flat, dark, bias
OBSERVAT	=	' '	/ observatory
START	=	'21:12:39.16309'	/ measurement start time (DMT) (hh:mm:ss.sssss)
EXPTIME	=	8.0058	/ actual integration time (sec)
CAMTEMP	=	-68.6050	/ camera temperature (C)
DETECTOR	=	'CCD4290 E2V'	/ detector
CAMERA	=	' '	/ CCD camera
RATE	=	2000	/ readout rate (KPix/sec)
GAIN	=	4.4	/ gain, electrons per adu
INTGAIN	=		/ internal gain
NODE	=	'All'	/ output node
BINNING	=	'1x1'	/ binning
PXSIZE	=	'13.5 x 13.5'	/ pixel size (mkm x mkm)
UT	=	' '	/ universal time (hh:mm:ss.sss)
ST	=	' '	/ local sidereal time (hh:mm:ss.sss)
RA	=	321.7613	/ Right Ascension (degrees)
DEC	=	60.5478	/ Declination (degrees)
EPOCH	=		/ EPOCH OF RA AND DEC
Z	=	36.119	/ zenith distance
A	=	229.3315	/ azimuth
PARANGLE	=		/ parallactic angle
ROTANGLE	=		/ field rotation angle
SEEING	=	' '	/ seeing
FILTER	=	' '	/ filter
FOCUS	=	1378.0	/ focus of telescope (mm)
IMSCALE	=	' '	/ image scale ("/Pix x "/Pix)
OUTTEMP	=	19.2	/ outside temperature (C)
WIND	=		/ wind (m/s)
CLOUDS	=		/ clouds (%)
PRESSURE	=	961.72	/ pressure (hP)
HUMIDITY	=	61.5	/ relative humidity (%)
DEBUG	=	0	/ 0 - work mode, 1 - debug mode

Table 2: Example of a FITS image header of the 75-cm telescope (continued)

```
OPU-TIME  =  '21:12:43.17999'  / time (hh:mm:ss.0000) from OPU
VALIDTM   =  3                 / 0 - no, 1 - VShV safe, 2 - MShV safe, 3 - yes
CCDNUM    =  3                 / CCD number
SAONUM    =  6                 / CCD number (SAO)
OPENBEG   =  '21:12:39.113'    / shutter begin open time (sec)
OPENEND   =  '21:12:39.212'    / shutter end open time (sec)
CLOSEBEG  =  '21:12:47.130'    / shutter begin close time (sec)
CLOSEEND  =  '21:12:47.207'    / shutter end close time (sec)
MREVERSE  =  0                 / blind movement:  0 - direct, 1 - reverse
OPU-Z     =  36.119            / zenith distance from OPU
OPU-A     =  229.3315          / azimuth from OPU
HISTORY
COMMENT
END
```

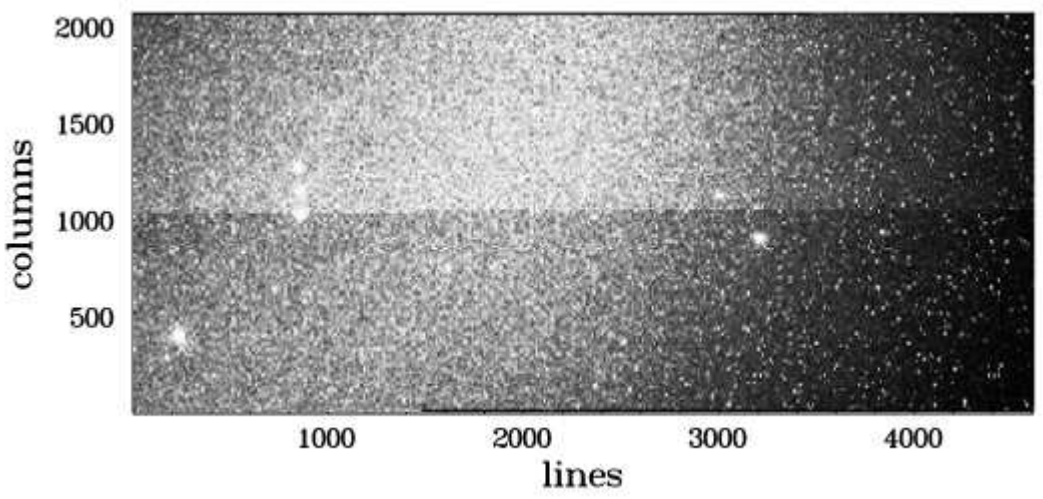

Figure 1: A single 8 sec exposure of SA-18 taken with the 75-cm telescope (rotated by 90^{o} for convenience).

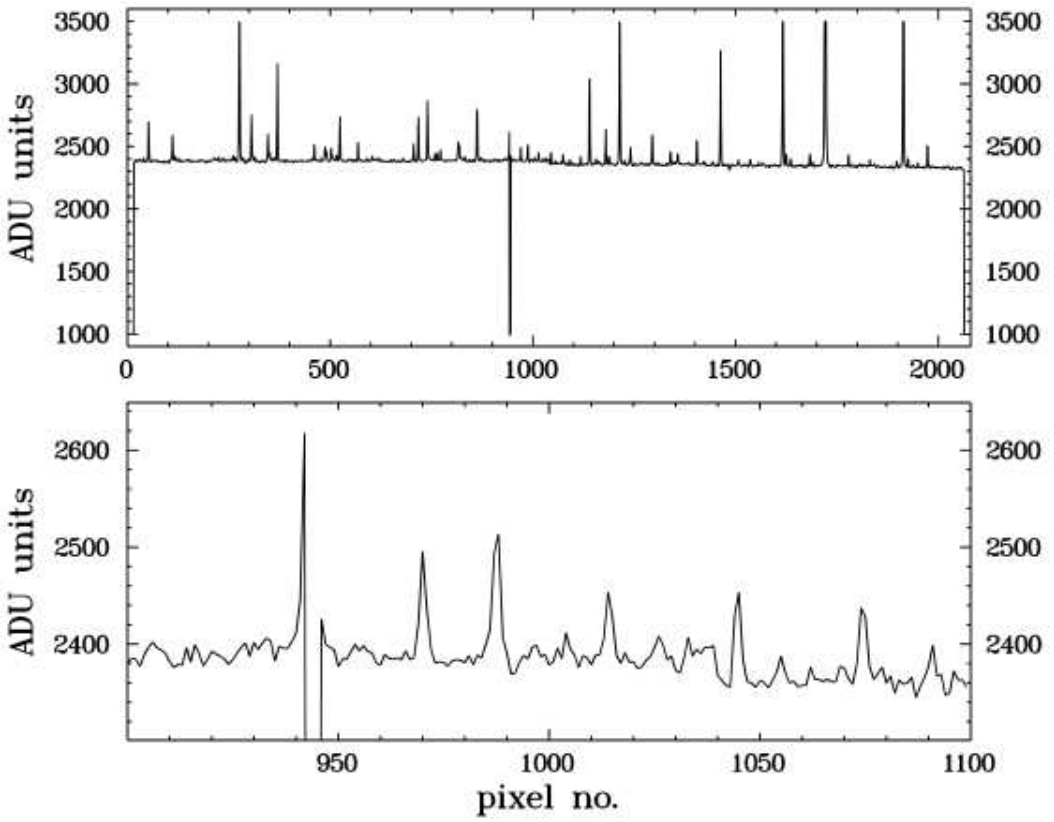

Figure 2: *Top:* Average of 10 lines close to the centre of the image shown in Fig. 1. The vertical spikes are due to stars in the field. They were truncated to 3500 ADU units. *Bottom:* An extended view of the central part of the graph shown in the upper panel.

Two characteristics are immediately obvious: (i) The image is divided into two sections. The background in the upper one appears to be higher than that in the lower section, suggesting that the sensitivity of the upper one is higher or that the bias level is different in the two sections. This may be caused by two different readout channels of the CCD. (ii) The variable background with a bright "blob" in the centre suggests that no flat field correction has been performed.

The intensity scale of the image in Fig. 1 was chosen such that the differences between the various sections of the image is maximized. In order to assess the real difference between the upper and lower sections Fig. 2 shows in the upper part a vertical cut through the image centre (average of 10 image columns).

The graph is characterized by a generally high count level, most of which probably represent the bias level of the CCD. The upward spikes are, of course, caused by stars in the field. They were truncated to 3500 ADU units. At the edges the count level drops, as it does for a few pixels close to the centre of the displayed range. The latter feature does not coincide with the border between the brighter and fainter sections in Fig. 1. It is probably due to some bad CCD columns[1].

[1]Therefore, this feature will probably not appear on data taken with the OPD-PanEOS complex (but, of course, similar detector flaws may occur).

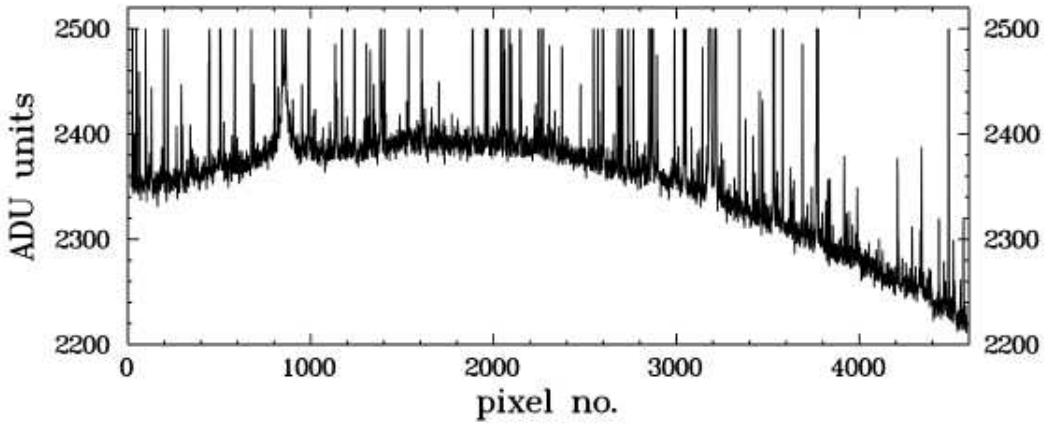

Figure 3: Average of 10 columns close to the bottom of the upper section of the image shown in Fig. 1. The vertical spikes are due to stars in the field. They were truncated to 2500 ADU units.

The border of the brighter and fainter sections is better visible in the lower frame of Fig. 2 which is an expanded view of the central part of the graph in the upper frame. Here, a systematic drop of the ADU units at pixels above pixel number 1040 with respect to lower pixel numbers can be seen. This is right in the middle of the CCD which has 2080 pixels in the respective direction. Sampling parts of the picture close to the borderline between the sections (and avoiding the bad columns), it is found that the difference between the medians of the ADU units[2] is 25.5 ± 2.4. This is of the order of 1% of the absolute ADU unit level.

Fig. 3 shows the average of 10 columns close to the bottom of the upper section of Fig. 1 in order to give an idea of the effect of the flat field. Again, the stars appear as truncated spikes. The systematic variation of the background, attributed to the flat field, has a modulation of about 7% of the average signal.

At the moment it is not clear if the basic corrections of bias and flat field are routinely applied to the PanEOS data. If this is the case, the above mentioned effects should easily be accounted for. Otherwise, they will represent a complication for the use the for data for astronomical purposes.

3.2 Plate scale and orientation

The image orientation is such that the long side of the CCD image (i.e., along the CCD lines) is roughly aligned with right ascension and the small side (i.e., along the CCD columns) with declination. However, the deviation from this rough alignment is considerable: a rotation by $106^{\circ}.4$ (counter-clockwise)[3] is required to bring the image into the standard orientation (north-south along the CCD lines; east-west along the CCD columns).

The pixel coordinates of two bright stars in the field together with their coordinates as quoted in astrometric catalogues[4] yield a plate scale of 2.0 "/pixel. Consequently the entire field of view encompasses $2^{\circ}.57$ (roughly in right ascension) $\times$ $1^{\circ}.16$ (roughly in declination)

[2]The median is expected to be less sensitive to the influence of stars than the mean.

[3]i.e., more than a rotation by 90° which would be necessary to transform the image to the standard orientation if lines and columns were perfectly aligned to right ascension and declination, respectively.

[4]For simplicity I used the AGK3 catalogue. Within the accuracy aspired in the present context the exact choice of the catalogue is irrelevant.

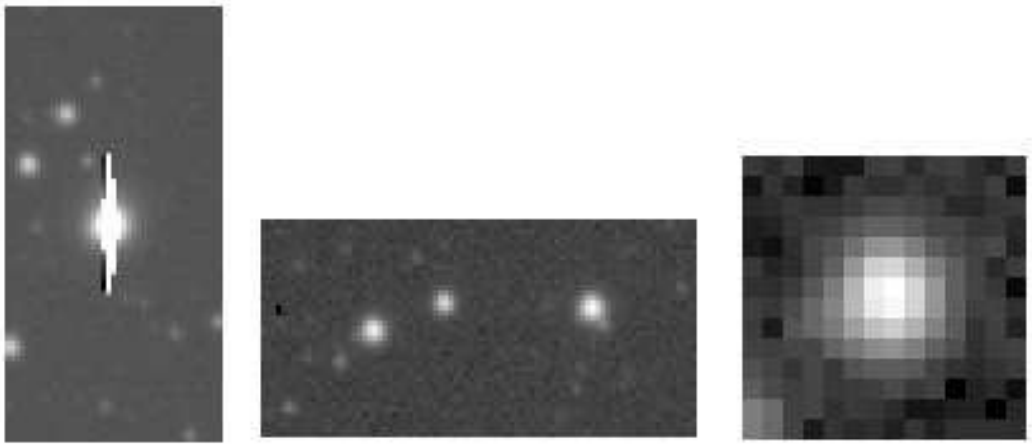

Figure 4: Details of an image taken with the 75cm telescope. On the left a bright, saturated star is shown. The image in the center contain some fainter star, and the image on the right contains a blown up vision of one of the star in the central image.

or almost exactly 3 square degrees on the sky.

3.3 Image resolution and quality

Starting to study the image shape and resolution, Fig. 4 shows three small sections of an individual image, exhibited on a logarithmic intensity scale. On the left a comparatively bright star is shown. There is obviously significant bleeding in the direction of the CCD columns. The centre of the star and much of the streak in the direction of the columns is saturated. The central image shows some fainter stars. Finally, the image on the right side is a blow-up of the left one of the three brightest stars of the central image.

In order to examine if distortions of the stellar images occur across the field of view of the telescope, contour plots were created for 25 stars distributed approximately in a 5×5 pattern across the images. They are shown in Fig. 5 where the lay-out follows the distribution of the respective star in the field of view (i.e., the central contour refers to a star close to the centre of the image, those in the edges to stars close the edges of the field of view).

There are no significant differences in the shape of the contours. If any, image distortions remain small even at the very edges of the images (but see below).

Another way to look at the same issue is to examine the width of the stellar profiles as a function of location on the image. For this purpose the same stellar images for which the intensity contours are shown in Fig. 5 were collapsed along the lines and the columns. The FWHM of a Gaussian fit to the resulting distribution (expressed in pixel units) is shown in Fig. 6. The results are arranged in a similar way as in Fig. 5: Each graph shown the FWHM for stars in five regions of image columns. In vertical direction they refer to five regions of image lines.

In this case some systematics can be seen. The FWHM in the direction of image lines increase systematically as a function of image column for all line regions (right hand side of Fig. 6). In the direction of image columns (left hand side of the figure) the FWHM also shows systematics trends with the image columns. However, this trend changes sign as a function of line region. As long as the FWHM in both direction (lines and columns) changes in the same way, the stellar profile will not change its shape but just becomes wider or

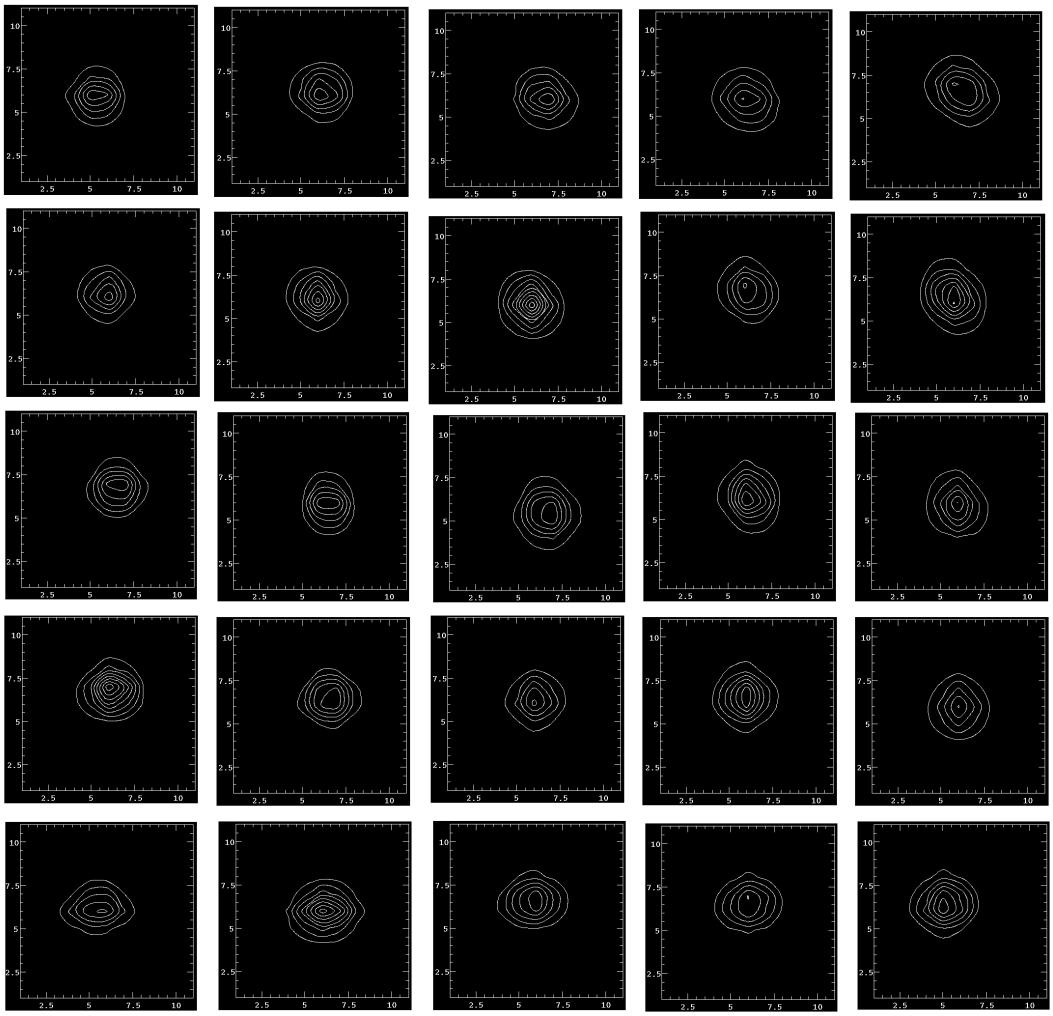

Figure 5: Intensity contours of star images distributed across the field of view of the 75cm telescope.

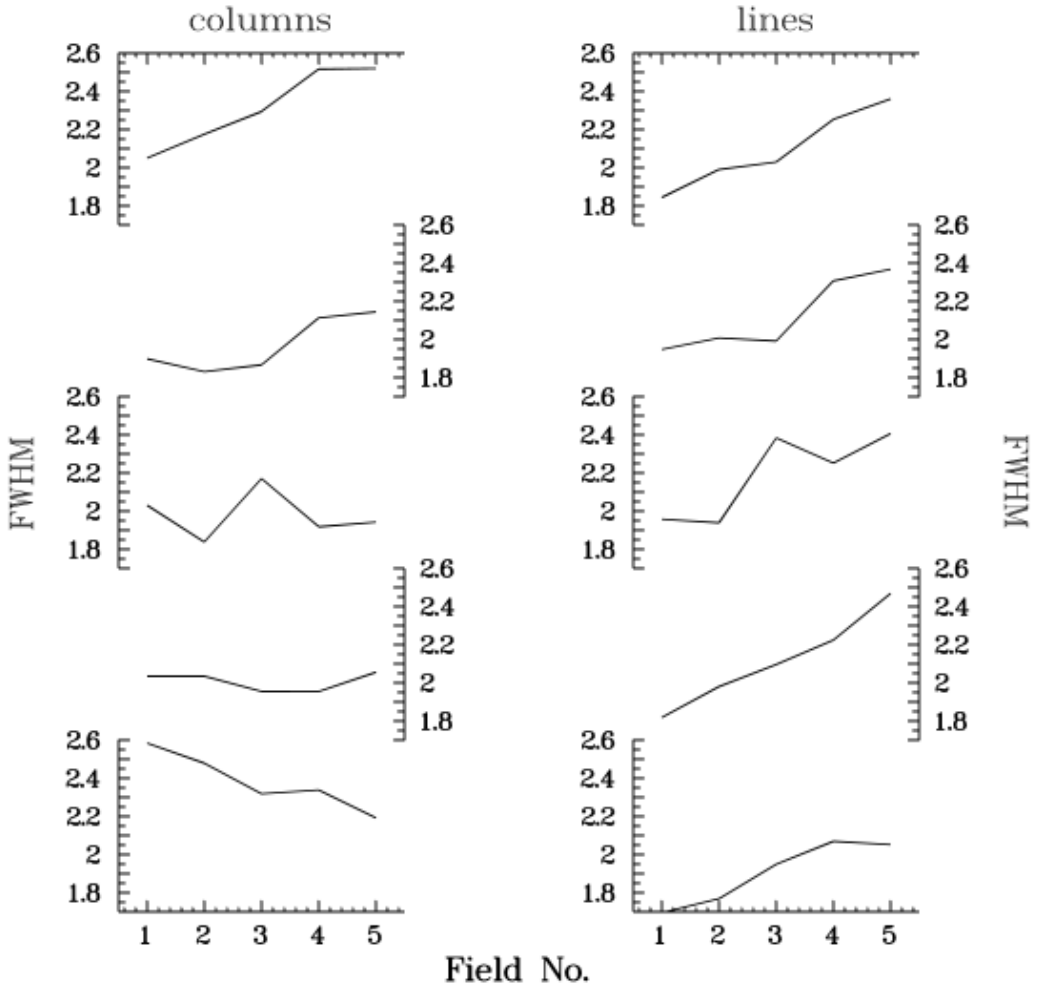

Figure 6: FWHM (in pixels) of the profiles of the stellar images along the CCD columns (left) and lines (right) as a function of their location within the field of view in five image sections in the directions of the columns (horizontal direction) and five sections along the columns (stacked graphs in vertical direction).

Table 3: Magnitudes of selected stars

No. (Fig. 7)	Designation (NOMAD catalogue)	B	V	R
1	1506-0304601	13.56	13.10	12.43
2	1506-0304597	15.90	15.72	15.80
3	1506-0304553	15.74	14.93	14.59
4	1506-0304622	17.75	17.04	16.75
5	1506-0304656	17.91	17.09	17.13

narrower. This is not the case when the change is different for lines and columns. Thus, Fig. 6 suggest that in the lower part of the CCD image the stellar profiles may change their shape as a function of location on the image, while in the upper part they just change their size.

3.4 Image depth

In order to assess the image depth (limiting magnitude) a small section of the image was selected. The respective stellar field of a single 8^{s} exposure is shown in the upper frame on the left side of Fig. 7. The intensity scale was chosen such as to maximize the visibility of faint stars[5]. The lower frame on the left side results from co-adding all ten 8^{s} exposure images of the field taken in immediate succession (see Table 2)[6]. As expected, more details are visible in the image after co-adding.

For comparison, the right side of Fig. 7 contains the same stellar field as it appears on digitalized POSS II plates in the blue (top) and red (bottom) spectral regions. While the resolution of the POSS II images is superior to that of their PanEOS equivalent, the limiting magnitude of the co-added PanEOS image – at least when compared to the red POSS II image – appears to be comparable.

A quantitative assessment of the limiting magnitude of the PanEOS images is hampered by the unknown statistical properties of the image (e.g., ADU conversion, bias level). Moreover, the expected high background contribution due to the full moon would lead to a brighter limiting magnitude than would be typical for a dark night. The PanEOS images being taken in white light further complicates the comparison with magnitudes in a specific photometric system.

In order to provide nevertheless an idea of the depth of the images, five stars in the field were identified with stars in the NOMAD catalogue (Zacharias et al., 2004). These are marked in the schematic representation in Fig. 7 (top). The BVR magnitudes as listed in the NOMAD catalogue are quoted in Table 3.

The two stars with roughly $V = 17$ (stars 4 and 5) appear to be close to the magnitude limit in the single exposure PanEOS image but are significantly brighter than the faintest stars visible in the co-added image. Considering also that the present images were obtained during bright moonlight it appears credible that the limiting magnitude of 19^{m} quoted in specification documents for PanEOS can indeed be achieved.

[5]The same is true for all other frames in Fig. 7.

[6]There is a slight positional shift between the individual exposures. This shift has been removed before coadding the images.

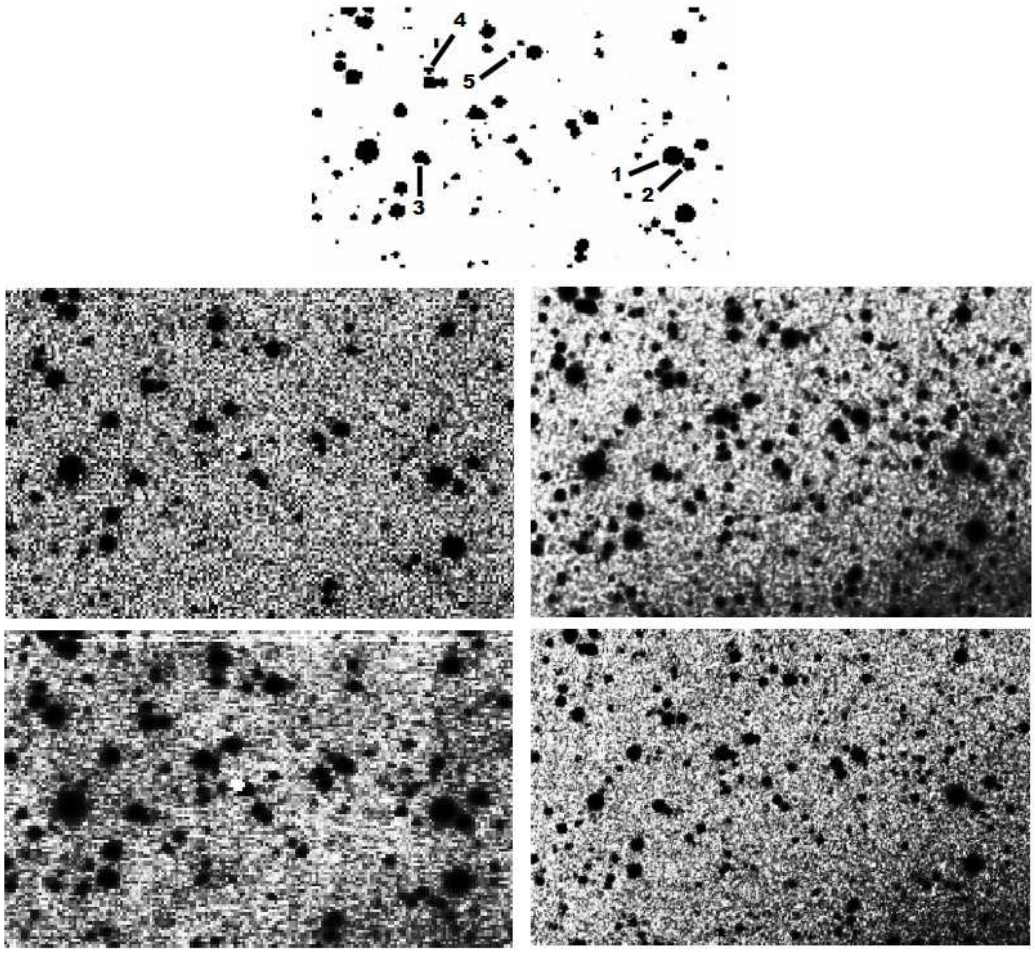

Figure 7: On the left side, the upper frame shows a small part of a single 8^s exposure image of the 75-cm telescope. The lower frame contains the same field, resulting from coadding ten 8^s exposures taken in immediate succesion. On the right side the same stellar field is shown as it appears in the digitalized POSS II sky atlas on blue (top) and red (bottom) plates. In the schematic representation of the field shown on top those stars are identified for which magnitudes are quoted in Table 3.

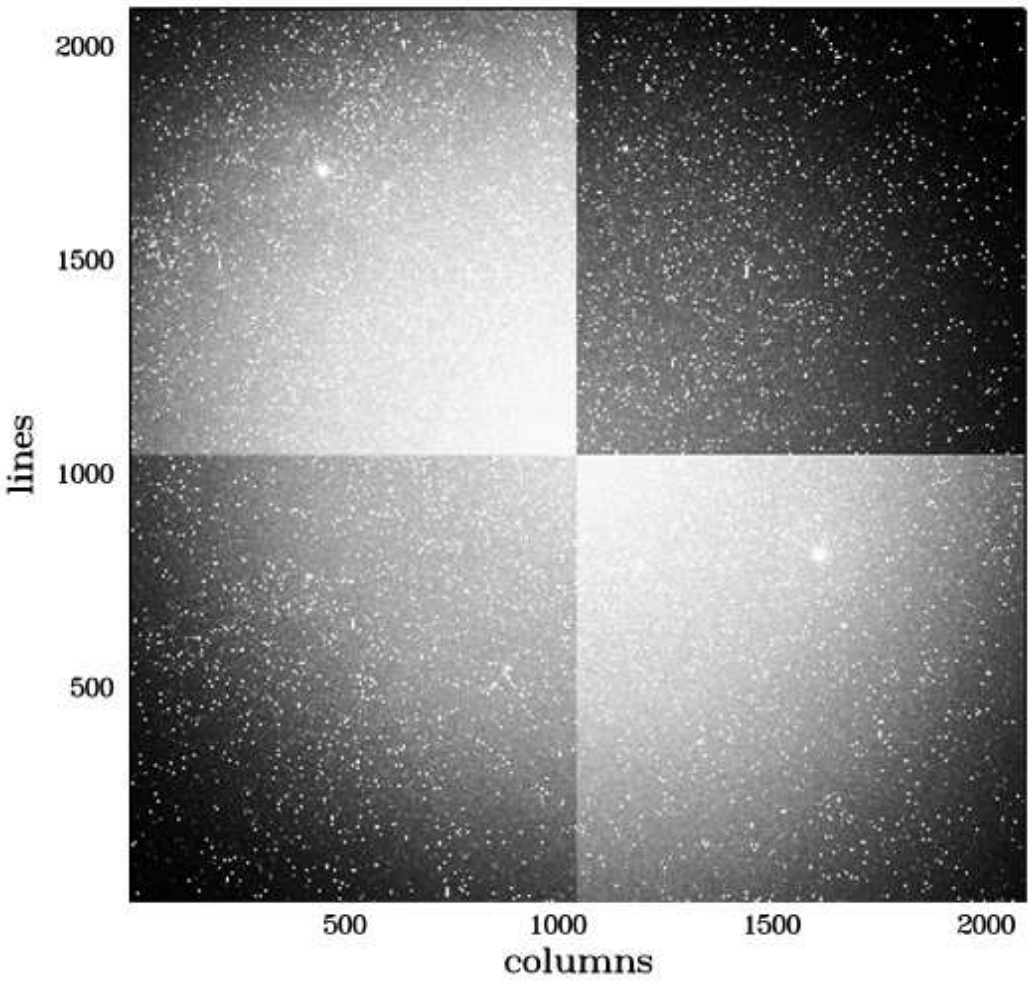

Figure 8: A single 10 sec exposure of SA-18 taken with the 25-cm telescope.

4 25-cm telescope data

The 25-cm telescope data will certainly not be as interesting for astronomical research by far when compared to the 75-cm telescope data. Therefore, I will content myself here to investigate only some basic characteristics. In particular, I will not assess the image quality and the depth.

4.1 General characteristics

Fig. 8 shows a single 10 sec exposure of a field centred on the same coordinates as the 75-cm telescope image reproduced in Fig. 1. It has a size of 2092×2092 pixels.

It is obvious that just as in the case of the 75-cm telescope the image is divided into several sections. Here, four sections of equal size can be distinguished. Again, it may be speculated that this is either due to detector parts with different sensitivities, bias levels or readout channels. Since there is no gap between the sections this effect is probably not due

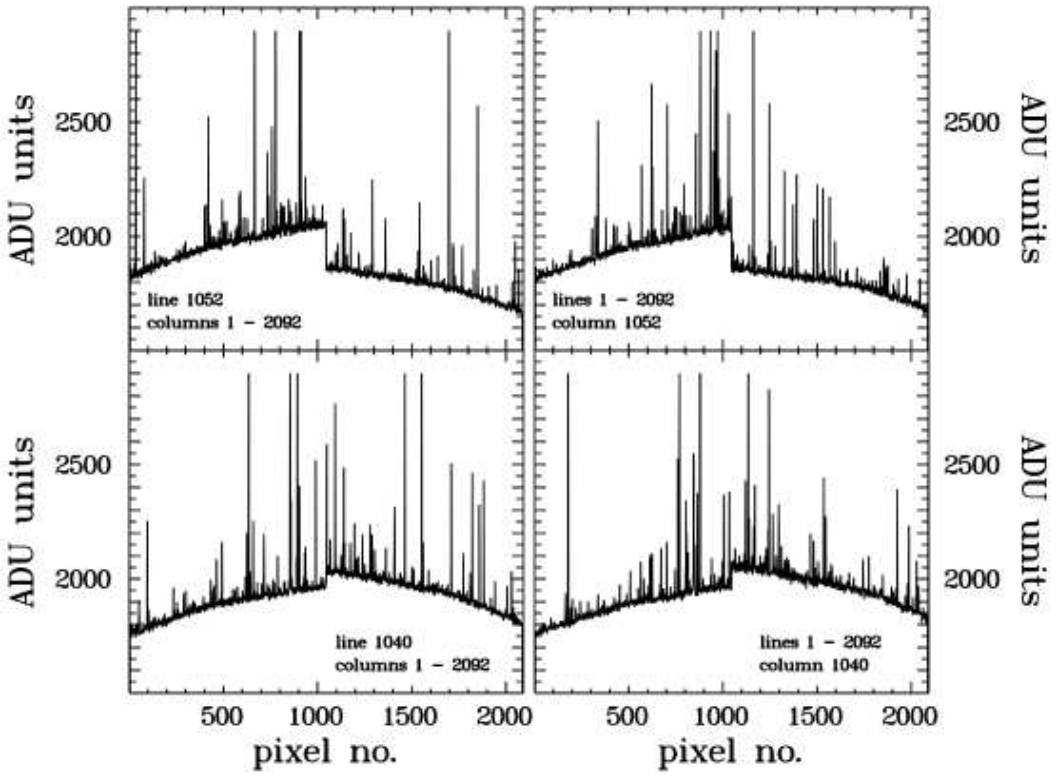

Figure 9: Cuts through the image shown in Fig. 8 close to the division between the various image sections. *Top left:* line 1052; *Bottom left:* line 1040; *Top right:* column 1052; *Bottom right:* column 1040. The vertical spikes are due to stars in the field. They were truncated to 2900 ADU units.

to the detector being composed of a mosaic of four different CCDs. Moreover, the bright "blob" concentrated to the centre of the image suggests again that no flat field correction has been performed.

In order to assess the difference in sensitivity (or bias level) between the parts of the detector, Fig. 9 shows four cuts through the image perform right below and right above, as well as just to the left and just to the right of the division between the image sections. Whereas in the 75-cm telescope image the difference between the two sections was found to be rather small (see Sect. 3.1), the steps between the sections is significantly more expressed in the present case.

4.2 Plate scale and orientation

The image orientation of the 25-cm telescope images is such that the CCD lines are roughly aligned with right ascension and the columns with declination. However, as in the case of the 75-cm telescope this alignment is not perfect. A rotation of $87^{\circ}.4$ is necessary to bring the image into the standard orientation (Sect. 3.2).

The plate scale is measured to be 11.9 "/pixel. Consequently, the image encompasses a field of approximately $6^{\circ}.9 \times 6^{\circ}.9 \approx 48^{\circ 2}$ on the sky.

The effect of the reduced image resolution of the 25-cm telescope when compared to that

Figure 10: Detail of an image taken with the 25-cm telescope showing the same field as the central frame of Fig. 4.

of the 75-cm telescope is illustrated in Fig. 10 which shown the same field as the central frame of Fig. 4, now observed with the smaller telescope.

5 Conclusions

This contribution is not meant as an exhaustive assessment of the capabilities of PanEOS for astronomical research. At the moment such an enterprise is still not possible in the absence of information available on observational procedures to be adopted for the PanEOS complex at OPD and because of the limited and not well documented data made available from the Altay PanEOS station. Therefore, I have restricted myself to an attempt to asses and, when possible, to quantify some basic characteristics of the data.

Whether or not the PanEOS images will indeed be useful for astronomy depends, of course, apart from the image quality and the strategy for their observations decisively on the research goal which must be defined by the potential users. Therefore, an unequivocal statement in the sense "Yes, the data are useful" or "No, the data are not useful" is not possible.

Even so, it is hoped that this contribution may provide a first indication for potential users whether or not it is worthwhile to think about possible scientific applications of the data that PanEOS will provide. A deeper study will be possible only after PanEOS starts its operations at OPD.

References

Zacharias, N., Monet, D.G., Levine, S.E., et al. 2004, Bull. AAS, 36, 1418